

Superconductivity and topological Fermi surface transitions in electron-doped cuprates near optimal doping

Tanmoy Das, R. S. Markiewicz, and A. Bansil

Physics Department, Northeastern University, Boston MA 02115, USA

(Dated: February 9, 2022)

We discuss evolution of the Fermi surface (FS) topology with doping in electron doped cuprates within the framework of a one-band Hubbard Hamiltonian, where antiferromagnetism and superconductivity are assumed to coexist in a uniform phase. In the lightly doped insulator, the FS consists of electron pockets around the $(\pi, 0)$ points. The first change in the FS topology occurs in the optimally doped region when an additional hole pocket appears at the nodal point. The second change in topology takes place in the overdoped regime ($\sim 18\%$) where antiferromagnetism disappears and a large (π, π) -centered metallic FS is formed. Evidence for these two topological transitions is found in recent Hall effect and penetration depth experiments on $\text{Pr}_{2-x}\text{Ce}_x\text{CuO}_{4-\delta}$ (PCCO) and with a number of spectroscopic measurements on $\text{Nd}_{2-x}\text{Ce}_x\text{CuO}_{4-\delta}$ (NCCO).

PACS numbers: 71.18.+y, 74.20.Rp, 73.20.Mf, 71.10.Hf

INTRODUCTION

An understanding of the origin of electron-hole asymmetry can provide important clues for unraveling the mechanism of pair formation in high- T_c superconductors. Our recent analysis[1, 2, 3] indicates that the electron doped cuprates behave like uniform antiferromagnetic metals and superconductors over a wide doping range up to a quantum critical point (QCP). As the half-filled state is doped, electrons condense into pockets around the $(\pi, 0)$ -points at the bottom of the upper magnetic band (UMB). With increasing doping the magnetic gap decreases, and as the lower magnetic band (LMB) crosses the Fermi level (E_F), hole pockets appear near the nodal regions, resulting in the first topological transition (TTI) of the Fermi Surface (FS). Here the nodal hole pockets coexist with the $(\pi, 0)$ electron pockets, separated by the hot-spot regions of the FS due to residual antiferromagnetism. With further electron doping, antiferromagnetic (AFM) order is destroyed as the magnetic gap collapses around $x \approx 0.18$, and the FS crosses over from being a collection of small pockets to a large metallic (π, π) -centered sheet, yielding the second topological transition (TTII) of the FS[4]. Our model of these two topological transitions in the FS is consistent with angle resolved photoemission spectroscopy (APRES)[5], resonant inelastic X-ray scattering (RIXS)[6] and other experimental results as discussed below.

It is interesting to ask how the aforementioned topological transitions manifest themselves in the superconducting properties of the cuprates. In this connection, we show that the FS topology is reflected directly in the T -dependence of the penetration depth λ : the behavior of λ crosses over from an apparent ' s' -wave (nodeless d -wave) form below TTI, to a mixed $d + s'$ -wave form above TTI, to a pure d -wave form above TTII, even though the underlying pairing symmetry remains d -wave at all dopings. The present article thus expands

on our earlier penetration depth study[3], which showed that a linear-in- T superfluid density $n_s \propto \lambda^{-2}$ originates in the hole pockets around the nodal points, and that the superfluid density of the electron pockets varies exponentially with T . n_s then appears nodeless in the underdoped regime due to strong AFM correlations. Near optimal doping, the appearance of the nodal pocket produces gapless hole quasiparticles which dominate at low T . Interestingly, with increasing T the small gap on the hole pocket is destroyed by thermal excitations and the system is left with a gap only on the electron pockets. The interplay between AFM order and superconductivity (SC) in determining how the SC pairing symmetry manifests itself in our calculations resolves a long standing controversy regarding the pairing symmetry in electron doped cuprates[7, 8, 9, 10, 11, 12, 13, 14, 15].

Recent Hall effect measurements[16, 17] provide further evidence for the existence of the TTI involving the appearance of nodal hole pockets around optimal doping. We show in this article that, above optimal doping, the experimentally observed crossover from a positive Hall coefficient at low T to negative at higher T is a direct consequence of the coexistence of two types of charge carriers. We also comment on possible consequences of the coexistence of the electron- and hole-like quasiparticles such as non-Fermi-liquid behavior[18] and Bose-Einstein condensation[19, 20].

MOTT INSULATOR TO MOTT GAP COLLAPSE

Our analysis proceeds within the framework of a one-band Hubbard Hamiltonian with tight-binding (TB) hopping parameters t, t', t'' , on-site repulsive interaction U , and a d -wave pairing interaction Δ ; see Refs. 2 and 3 for details. Mean field Hartree-Fock approach is used to solve for all the order parameters self-consistently in the AFM, normal as well as the SC states, assuming that the

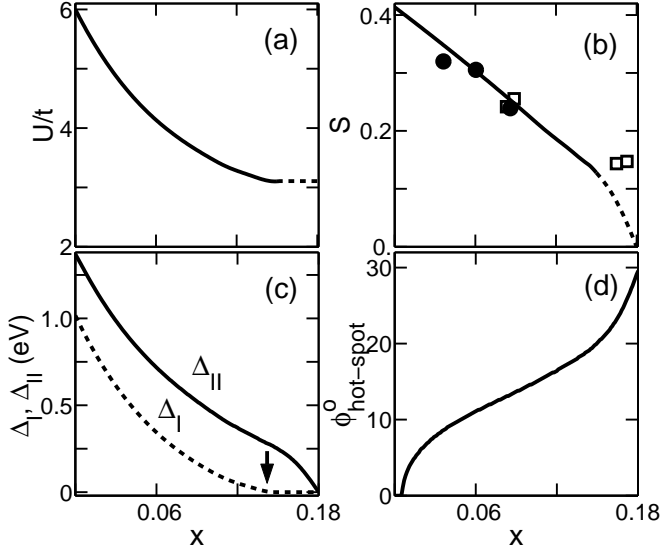


FIG. 1: (a) Doping dependence of U/t . (b) Self-consistently computed magnetisation, S , (solid line, extrapolated and shown dashed at higher dopings as it terminates in a QCP) and the corresponding experimental results from Ref. 21 (open squares) and Ref. 22 (filled dots). (c) Nodal point pseudogap (Δ_I), defined as the energy gap from the E_F to the LMB at the nodal point, is plotted as a function of doping in dashed line. The arrow marks the doping ($x = 0.145$) where this pseudogap vanishes at the first topological transition TTI. Hot-spot gap (Δ_{II}) is shown in solid line which terminates near 18% doping, denoting the second topological transition, TTII. (d) The position of the hot-spot gap is given by the FS angle, $\phi_{\text{hot-spot}}^o$; the angle is zero (45°) along the antinodal (nodal) direction.

effective U is doping dependent as shown in Fig. 1(a). U varies rapidly at low dopings, but the doping dependence is much weaker at higher dopings[4]. A finite expectation value of the staggered magnetization S at the nesting wave vector $\vec{Q} = (\pi, \pi)$ produces a gap in the low energy spectrum in a mean field treatment. S is seen from Fig. 1(b) to decrease linearly with doping up to optimal doping and to then drop sharply, disappearing around $x = 0.18$, even though U is nearly doping independent at higher dopings. Incidentally, we adduce that the values of the TB parameters and U , and thus of S are quite similar in NCCO[1] and PCCO[3], although $\text{Pr}_{1-x}\text{LaCe}_x\text{CuO}_{4-\delta}$ (PLCCO) seems to be somewhat different[2]. The magnetic gap given by US splits the bare band into the upper (UMB) and lower (LMB) magnetic bands, where at half-filling, the LMB is fully occupied and the UMB is empty. A gap between the E_F and the top of the LMB at the nodal point would result in a nodal pseudogap (Δ_I) in the spectrum when fluctuation effects missing in our mean field computations are accounted for. This nodal pseudogap is seen from Fig. 1(c) (dashed line) to have a large value of 1.0 eV at half filling, and to close at the TTI. In contrast, the pseudogap at the hot-spot (Δ_{II}), computed by the maximum gap in the FS, is larger than the nodal

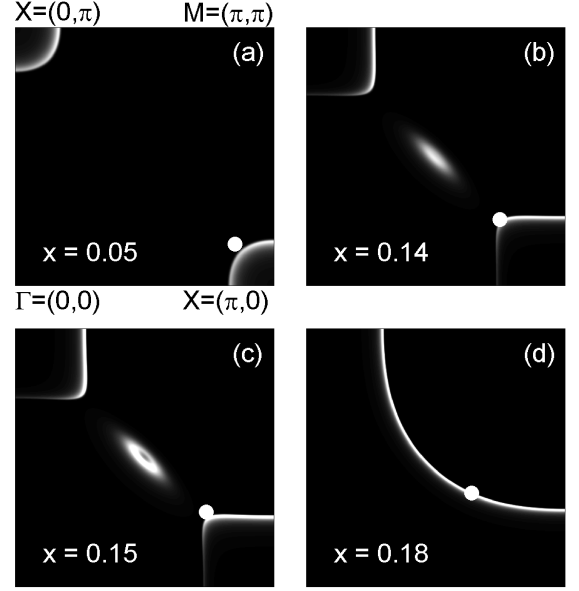


FIG. 2: Computed spectral intensity at the Fermi energy in PCCO, which gives an impression of the FS at different dopings. In (b), even though the LMB is below the E_F , some intensity can be seen around the nodal point due to the integration of the spectral intensity over a finite energy window around E_F (to mimic experiment). Whites denote high and blacks low intensity. The dots mark the positions of the hot-spot as discussed in Fig. 1(c)-(d); and the dot in (d) represents the limiting value of momentum where hot-spot disappears

pseudogap (shown by the solid line), and closes at the QCP (i.e. TTII). The position of the maximum hot-spot gap is represented by the FS angle ($\phi_{\text{hot-spot}}^o$) in Fig. 1(d), where the angle is zero (45°) along the antinodal (nodal) direction. Interestingly, the hot-spot in electron doped cuprates appears in the antinodal direction at half filling. A similar behavior is also seen in the hole doped case[23]. With increasing doping, the gap moves away towards the nodal direction nonlinearly with doping, where for hole doped cuprates, it stays at the antinodal direction for all dopings. The white dots in Fig. 2 mark the same $\phi_{\text{hot-spot}}^o$ on the FS maps at different dopings.

Turning to the computational details of the doping evolution of the FS, when the insulator is doped with electrons, the FS first forms as small, nearly circular electron pockets centered at $X = (\pi, 0)/(0, \pi)$, leading to an AFM metal as shown for $x = 0.05$ in Fig. 2(a). With increasing doping, these electron pockets become more squarish in shape, and lose spectral weight along the $\Gamma \rightarrow X$ direction as seen in Fig. 2(b). As we approach optimal doping, the nodal pseudogap vanishes around $x = 0.145$ (marked by the arrow in Fig.1(c)) as the LMB crosses E_F , producing the necklace-like FS of Fig. 2(c). Finally, a complete metal-like FS is restored in Fig. 2(d) as the magnetic gap collapses around $x = 0.18$.

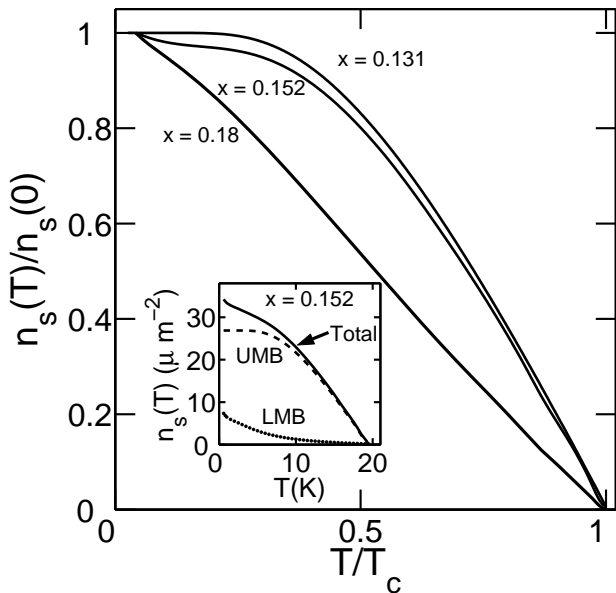


FIG. 3: Computed values of the normalized superfluid density $n_s(T)/n_s(0)$ as a function of scaled temperature T/T_c at three different dopings in PCCO [15]. $n_s(0)$ is the superfluid density at $T = 0$ and T_c is the SC transition temperature. *Inset*: Total n_s at $x = 0.152$ is shown decomposed into UMB and LMB contributions.

SUPERCONDUCTIVITY AND PENETRATION DEPTH

The superfluid density $n_s \propto \lambda^{-2}$ is a fundamental property of the superconductor and its evolution with doping provides insight into the interplay between the AFM and SC orders. The low- T behavior of n_s is traditionally used to determine the pairing symmetry[24], but results in electron-doped cuprates have been contradictory. Some early measurements found evidence for s -wave pairing[7, 8], but other tunneling[12] and penetration depth[13, 14] experiments report d -wave pairing. Yet other experiments suggest a transition from an s -wave in underdoped samples to either a d -wave[9, 10] and/or a mixed ($d + is$)-wave[11] character in the optimally and overdoped cases.

We have addressed this issue by directly calculating the penetration depth in a model with coexisting AFM and SC orders, assuming d -wave pairing at all dopings. The technical details of the calculations and the corresponding doping dependent SC order parameters are given in Ref. 3. Typical results for the superfluid density n_s are given in Fig. 3, and show that it varies exponentially in the underdoped region at $x = 0.131$, even though the pairing symmetry is d -wave. This is due to the absence of spectral weight in the nodal region associated with the large nodal pseudogap. In contrast, in the optimal doping region at $x = 0.152$ [25], n_s shows a linear-in- T behavior in the very low- T region ($T < 1.5K$) as the nodal hole pocket is formed (see inset in Fig. 3). Inter-

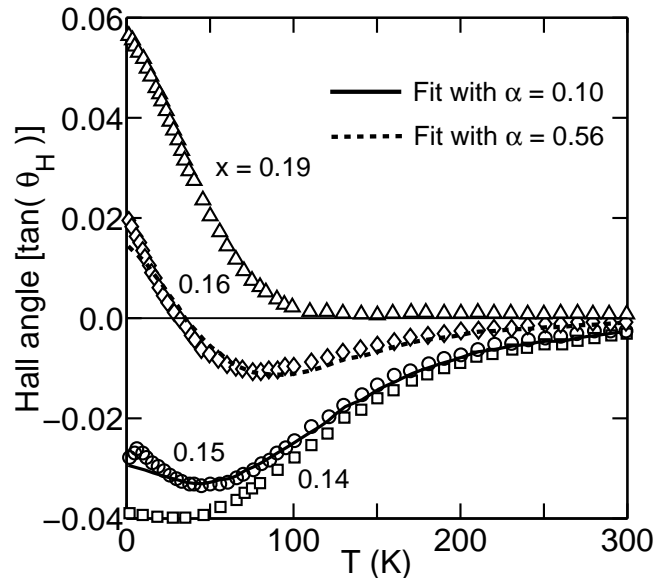


FIG. 4: Experimental values of the Hall angle θ_H [17] as a function of T at several dopings. Solid and dashed lines through the data for $x = 0.15$ and $x = 0.16$, respectively are qualitative fits of form $[\alpha\theta_H(x = 0.19) + (1 - \alpha)\theta_H(x = 0.14)]$, where α is a mixing parameter.

estingly, for higher T , the theoretical penetration depth shows a transition from a linear-in- T to an exponential in accord with experimental observations[15].

To clarify the complicated T -dependence of n_s , we have investigated the partial contributions to the total superfluid density from the UMB and LMB at $x=0.152$ and the results are summarized in the inset in Fig. 3. Since the UMB lies well above the nodal point at all dopings, the associated contribution displays an apparent ' s '-wave like behavior (dashed line in the inset). Once the nodal pocket is formed the LMB contributes a linear-in- T behavior (short dashed line). But at $x=0.152$, this hole pocket is quite small, and hence the linear-in- T behavior persists only at very low T . At high T the electron quasiparticles dominate, yielding to an ' s '-wave-like plateau in the total superfluid density (solid line). This leads to an apparent mixed $d + s'$ -wave like behavior in the pairing symmetry.

A second transition is expected in the overdoped regime near $x = 0.18$, where the magnetic gap collapses and only a single large FS sheet remains. This transition should be clearly observable in penetration depth as seen from the dashed curve in Fig. 3 in which there is no trace of the ' s '-wave like plateau. So far, however, experimental data has to our knowledge not been reported on such highly doped samples. It is clear thus that the doping evolution of n_s provides a direct handle on the topology of the underlying FS.

TRANSPORT PROPERTIES

Dagan *et. al.* [16, 17] have shown in PCCO that the Hall coefficient (see Fig. 4), R_H , as well as the Hall angle, θ_H , defined as $\tan(\theta_H) = \rho_{xy}/\rho_{xx}$, where ρ_{xy} (ρ_{xx}) denotes transverse (longitudinal) resistivity in the CuO_2 plane, crosses over from a negative to a positive value near optimal doping, implying that the charge character of the carriers changes from being electron-like in the underdoped system to becoming hole-like upon overdoping. For doping $x \leq 0.14$ the T -dependence of θ_H is seen in Fig. 4 to be monotonic and electron-like, while for $x = 0.19$ it is also monotonic but hole-like. For intermediate dopings, as illustrated by the data for $x=0.15$ and 0.16 , it is non-monotonic and may change sign with increasing T , from being hole-like at low T to electron-like at high T . Curiously, the Hall data at intermediate dopings can be fitted reasonably via a weighted average of the experimental data at low and high doping, some discrepancies notwithstanding. Specifically, the solid line in Fig. 3 through the $x=0.15$ data points corresponds to a superposition involving 90% of the $x=0.14$ data and 10% of the $x=0.19$ data in the figure. The dashed line for the $x=0.16$ dataset similarly corresponds to an admixture with 44% of the $x=0.14$ and 56% of the $x=0.19$ dataset. These observations leave little doubt that the intermediate doping regime involves two carrier conduction. Note that the onset of two-carrier conduction falls at essentially the same doping at which the nodal pockets first appear (i.e. TTI) as determined from penetration depth experiments. Very recently Li *et. al.*[26] have shown, using a spin density wave model similar to ours, that a FS crossover from a single electron-like FS to electron- and hole-like pockets is consistent with an anomalous non-linear magnetic field dependence of the high field Hall resistivity.

DISCUSSION AND CONCLUSION

The importance of topological transitions in controlling the properties of electron-doped cuprates has been considered by other authors. Krotkov *et. al.*[18] have shown that above what we have referred to as TTI the low energy spin dynamics is dominated by gapless bosonic collective modes near the nodal point. This causes the holes to develop a large mass, so that the resulting *heavy fermion* behavior can alter the fermionic dynamics and may lead to non-Fermi-liquid effects, including anomalous frequency dependencies of the conductivity and Raman response. They also argue that the strong reduction of T_c in electron-doped cuprates compared to the hole-doped case is a reflection of differences in the FS topology. Another interesting consequence of the co-existence of two carriers near optimal doping could be a BCS to Bose-Einstein condensation (BEC) crossover.

The generalized BEC theory[20], which includes the co-existence of two-electron ($-2e$) and two-hole ($2e$) Cooper pairs associated with separate bands, suggests the possibility that bosonic electron-hole pairs could undergo Bose condensation[19, 20].

In conclusion, we have shown that our model of a uniformly doped antiferromagnetic metal/superconductor is capable of describing the doping evolution of a number of properties of the electron-doped cuprates. Our model fundamentally involves the presence of two distinct topological transitions of the FS, which are referred to as TTI and TTII here. The existence of TTI (appearance of nodal hole pockets) in the optimal doping region is indicated quite clearly by the penetration depth and Hall effect experiments. TTII (merging of the hole and electron pockets into a single large FS) lies close to the solubility limit of the material and would be more difficult to observe.

This work is supported by the U.S.D.O.E contracts DE-FG02-07ER46352 and DE-AC03-76SF00098 and benefited from the allocation of supercomputer time at NERSC and Northeastern University's Advanced Scientific Computation Center (ASCC).

-
- [1] C. Kusko, *et. al.*, Phys. Rev. B. **66**, 140513(R) (2002).
 - [2] Tanmoy Das, R. S. Markiewicz, and A. Bansil, Phys. Rev. B. **74**, 020506(R) (2006).
 - [3] Tanmoy Das, R. S. Markiewicz and A. Bansil, Phys. Rev. Lett. **98**, 197004 (2007).
 - [4] We have extrapolated our order parameters to the overdoped region and carried out self-consistent calculations to estimate the QCP.
 - [5] N. P. Armitage, *et. al.*, Phys. Rev. Lett. **87**, 147003 (2001).
 - [6] R.S. Markiewicz and A. Bansil, Phys. Rev. Lett. **96**, 107005 (2006).
 - [7] S. M. Anlage, *et. al.*, Phys. Rev. B. **50**, 523 (1994).
 - [8] S. Kashiwaya *et. al.*, Phys. Rev. B. **57**, 8680 (1998).
 - [9] J. A. Skinta, *et. al.*, Phys. Rev. Lett., **88**, 207005 (2002).
 - [10] A. Biswas, *et. al.*, Phys. Rev. Lett. **88**, 207004 (2002).
 - [11] M. M. Qazilbash, *et. al.*, Phys. Rev. B. **68**, 024502 (2003).
 - [12] B. Chesca, *et. al.*, Phys. Rev. B. **71**, 104504 (2005).
 - [13] A. Snezhko, *et. al.*, Phys. Rev. Lett. **92**, 157005 (2004).
 - [14] Ariando, *et. al.*, Phys. Rev. Lett. **94**, 167001 (2005).
 - [15] M.-S. Kim, *et. al.*, Phys. Rev. Lett., **91**, 087001 (2003).
 - [16] Y. Dagan, *et. al.*, Phys. Rev. Lett. **92**, 167001 (2004).
 - [17] Y. Dagan, and R. L. Greene, Phys. Rev. B **76**, 024506 (2007).
 - [18] P. Krotkov and A.V. Chubukov, Phys. Rev. Lett. **96**, 107002 (2006); Phys. Rev. B **74**, 014509 (2006).
 - [19] A. Brinkman, and H. Hilgenkamp, Physica C **422**, 71 (2005).
 - [20] S.K. Adhikari, *et. al.*, Physica C, **453**, 37-45 (2007).
 - [21] P. K. Mang, *et. al.*, Phys. Rev. Lett. **93**, 027002 (2004).
 - [22] M. J. Rosseinsky *et. al.*, Inorg. Chem. **30**, 2680 (1991).
 - [23] Tanmoy Das, R. S. Markiewicz, and A. Bansil,

- arXiv:0711.0480.
- [24] M. Prohammer and J. P. Carbotte, Phys. Rev. B. **43**, 5370 (1991).
- [25] Different groups find somewhat different dopings for optimal T_c , e.g. M.-S. Kim *et. al.*, [15] reports optimal doping near $x \approx 0.137$ for PCCO, where M. M. Qazilbash *et. al.*, Phys. Rev. B. **72**, 214510 (2005) reports the optimal doping near $x \approx 0.145$ in both PCCO and NCCO.
- [26] Pengcheng Li, F. F. Balakirev, and R. L. Greene, Phys. Rev. Lett. **99**, 047003 (2007).